Annals of Biomedical Engineering, Vol. 24, pp. 139–147, 1996
Printed in the USA.

0090-6964/96 $10.50 + .00

Three-Dimensional Reconstruction of the Flow in a Human Left Heart by Using Magnetic Resonance Phase Velocity Encoding

PETER G. WALKER,* GREGORY B. CRANNEY,† RANDALL Y. GRIMES,* JASON DELATORE,* JOSEPH RECTENWALD,* GERALD M. POHOST,‡ and AJIT P. YOGANATHAN*

*School of Chemical Engineering, Georgia Institute of Technology, Atlanta, GA; †Department of Cardiology, Prince Henry Hospital, Little Bay, Australia; and ‡Division of Cardiovascular Disease, Center for NMR Research and Development, University of Alabama at Birmingham, Birmingham, AL

Abstract—Intraventricular flows have been correlated with disease and are of interest to cardiologists as a possible means of diagnosis. This study extends a method that use magnetic resonance (MR) to measure the three-dimensional nature of these flows. Four coplanar, sagittal MR slices were located that spanned the left ventricle of a healthy human. All three velocity components were measured in each slice and 18 phases were obtained per beat. With use of the MR magnitude images, masks were created to isolate the velocity data within the heart. These data were read into the software package, Data Visualizer, and the data from the four slices were aligned so as to reconstruct the three-dimensional volume of the left ventricle and atrium. By representing the velocity in vectorial form, the three-dimensional intraventricular flow field was visualized. This revealed the presence of one large line vortex in the ventricle during late diastole but a more ordered flow during early diastole and systole. In conclusion, the use of MR velocity acquisition is a suitable method to obtain the complex intraventricular flow fields in humans and may lead to a better understanding of the importance of these flows.

Keywords—Magnetic resonance, Computer reconstruction, Velocity, Left ventricle.

INTRODUCTION

Intraventricular blood flow patterns have been correlated with cardiac disorders, such as ischemia (2,4–6,8,22), cardiomyopathy (10), and thrombosis (15), and, therefore, are a possible means of assessing cardiac function. One goal of clinical cardiology, therefore, is to find a method that can accurately measure the complex three-dimensional flow in a human ventricle to fully understand this relationship and to develop possible diagnostic techniques. To date, a number of approaches have been taken to achieve this goal including color Doppler (8,10), M-mode (22), B-mode (2,15), and pulse wave (2,4–6) ultrasound; computational modeling in conjunction with cine-angiography (1,20,21); and purely computational simulations (13,15,17,20,21). For various reasons, none of these methods is ideal for measuring the full three-dimensional, temporal variations in the intraventricular velocity over the cardiac cycle and throughout the entire ventricle. For instance, ultrasound cannot easily measure more than one component of velocity and requires translation or rotation of the ultrasound transducer to acquire images in more than a single plane. Computational methods that use the ventricular wall motion derived from cine-angiography have been used to study systolic flows only (9,24), and purely computational models are either too simplified (16,17) to produce a realistic flow field or too complex (13,18,28), requiring restrictive amounts of computer time.

However, recent developments in magnetic resonance imaging (MRI) have shown that it is possible to measure the three-dimensional velocity in a MRI slice through a human subject, making MRI a means of obtaining the intraventricular flow field. By triggering the MRI acquisition from the subject's electrocardiogram (ECG), temporal changes in velocity can be obtained. In addition, the MRI slice can be orientated in any direction, thereby, allowing imaging of any part of the body. These techniques previously have been applied to measure the flow in the ventricle through the acquisition of a single MRI slice (10,25). These studies were able to visualize and quantify the intraventricular flow field, including vortex formation and separation. The objectives of the work presented herein were to develop a method for expanding this single slice approach to a multislice acquisition in which the flow in the entire ventricle is measured and to visualize this volumetric velocity data in a meaningful manner. Such an acquisition should then provide a complete visualization of the intraventricular flow field and may lead to a better understanding of cardiac hemodynamics.

METHODS

The MRI acquisition was performed on a healthy 21-year-old man with no previous history of cardiac disease.

Acknowledgment—This work was supported by a grant from the American Heart Association, Georgia Affiliate.

Address correspondence to Ajit P. Yoganathan, School of Chemical Engineering, Georgia Institute of Technology, Atlanta, GA 30332-0100, U.S.A.

(Received 20Mar95, Revised 4Aug95, Revised, Accepted 15Sep95)

The subject was placed in a Philips (Philips Medical Systems, Shelton, CT) 1.5 Tesla, S-15 MR scanner in the supine position. A series of transverse spin echo scout images covering the subject's chest region were obtained to locate the position of the heart. With the use of these scout images, which showed the left ventricle in a short axis view, four sagittal slices 10 mm apart (center line to center line) were located so as to span the left ventricle throughout the cardiac cycle, (Fig. 1). Phase velocity was then encoded with the use of the FLAG pulse sequence 911) to obtain the velocity in three perpendicular directions in the sagittal slices. This gradient echo sequence used bipolar gradients to produce one velocity-compensated and three velocity-encoded images, one for each velocity direction. During measurement, the velocity-encoded and velocity-compensated sequences were interleaved at each encoding step (11). The final three velocity images were obtained by subtracting the velocity-compensated image from each of the velocity-encoded images. The slices obtained were 6 mm thick with a 128 × 128 resolution and a field of view of 280 mm, giving a pixel size of 2.19 × 2.19 mm. The velocity range was set at ±100 cm/sec and two signal averages were taken. The acquisition was triggered from the R-wave of the subject's ECG, allowing 18 images or cardiac phases (35 msec apart and equal to the repetition time) to be obtained throughout the cardiac cycle. The heart rate was 75 beats per min.

Velocity was measured with MRI by utilizing the degree of precession of the protons in the image. The rate of precession of the protons was proportional to the strength and direction of the applied magnetic gradient. When a positive magnetic gradient was applied, all protons preceded an amount that depended on the duration and local strength of the magnetic field. When an equal but negative gradient was then applied, stationary protons preceded the same amount but in the opposite direction. These stationary protons, therefore, had no net rotation or zero phase at the end of the procedure. When, on the other hand, the proton was moving during the application of the gradients, then it experienced a different magnetic field strength during the application of the positive and negative gradients. Its forward and backward rotation, therefore, differed, giving it a net rotation or phase at the end of the procedure. It can be shown that this net phase is proportional to the velocity, acceleration, and higher order motions of the protons. Under normal physiological conditions, however, the contribution to the phase from the acceleration and higher orders of motion can be neglected, leaving the phase directionally proportional to the velocity. In this way, the velocity in each voxel in an image can be obtained.

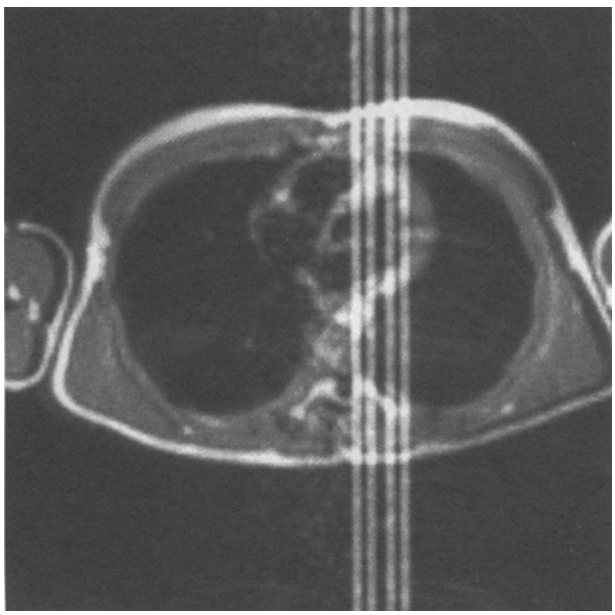

FIGURE 1. Transverse scout image showing the positioning of the sagittal velocity slices over the left ventricle.

A number of authors have validated the accuracy of MRI phase velocity encoding *in vitro* (14,19) by comparing it to computational (23) and laser Doppler anemometry (26). In addition, MRI has been shown to be accurate to within 5% when used to calculate the flow rate downstream of artificial heart valves (27). *In-vivo* validation of MRI is more difficult because of the lack of a gold standard for *in vivo* velocity measurements. However, comparisons between pulse Doppler ultrasound and MRI have been shown to give good agreement (7,12).

DATA ANALYSIS

The data obtained from the MR scans were transferred to a Silicon Graphics ONYX computer for analysis and visualization. The MR images obtained with a 280-mm field of view covered a significant portion of the chest; therefore, the first step in the data analysis was to extract from all images a smaller region covering the heart only. The next step was to create mask images. For each slice and cardiac phase, a mask image composed of zeros and ones was created manually in which ones were located inside the left ventricle and atrium, and zeros were located elsewhere. These images were created with the visualization software Spyglass Transform (Spyglass Inc., Savoy, ILL) and by using the magnitude images to show the anatomy. After generation of the mask images, they were multiplied by the corresponding velocity images to zero the velocity measurements outside the heart. The final phase in the data analysis was to format the data for input into the visualization software.

DATA VISUALIZATION

The three-dimensional visualization package used to perform the final reconstruction and animation of the flow

was Data Visualizer (Wavefront Technologies, Santa Barbara, CA). Numerous tools were used in this package. First, the outline of the ventricle and atrium was visualized by using cut planes placed coplanar with the MR slices. A cut plane is an imaginary slice through the data block in which vector and/or scaler data can be visualized in a number of ways. By using the computer mouse, this slice can then be moved and rotated through the data to visualize different regions. Within each cut plane, a contour of the mask data was generated, representing the outline of the ventricle and atrium. The outline was found by setting the contour's value to 0.5, which separated the ones within the ventricle and atrium from the zeroes outside. Second, the velocity normal to the MR slices (roughly atrial-apical direction) was visualized by representing it in raster form at the level of each of the MR slices. Finally, all three velocity components were visualized with vectors. All images were generated throughout the cardiac cycle and animated.

RESULTS

Figure 2 shows the magnitude images 12 msec after the R-wave (the start of systole) for the four sagittal velocity-encoded slices. On each of the images, the back of the subject is on the right with the left ventricle at the middle right of each image. The images progress from the patient's left (Fig. 2.1) to right (Fig. 2.4) covering the heart. The leftmost image, therefore, cuts the ventricle toward the apex, showing a small section of the papillary muscles, whereas the rightmost image cut the ventricle toward the septum and aortic valve, showing some of the ascending aorta and including part of the left atrium. The process of masking the region outside the heart was performed by using these and similar magnitude images. This is possible because of the difference in signal intensity between flowing blood and static tissue, as is clearly shown in Fig. 2.1. Unfortunately, this contrast was not always strong enough to provide a sharp border, which occasionally made it difficult to identify the inner ventricular boundary. Furthermore, it often was difficult to identify the boundary between the left atrium and ventricle.

In Fig. 3, cut planes were placed coincident with the MR slice, and the through-plane velocity was represented in raster format. With this type of representation, the magnitude of the velocity at each voxel in the MRI slices was given a color value (blue and red for apically and basally directed flows, respectively), the brightness of which increased with the velocity magnitude. The outlines of the raster images are the contours showing the inner wall of the heart. The apex of the heart is seen on the left of the images, and the left ventricular outflow tract (LVOT) is at the top right. Because of the orientation of the slices, the left atrium also is included and is shown at the front right of the images.

Figure 3a shows the visualized data during peak systole. From the almost total red color of the through-plane velocity, the image shows that the flow converged toward the aortic valve from the entire ventricle. The maximum velocity occurred in the LVOT. Within the atrium, there was flow toward the ventricle, as indicated by the blue color. Figure 3b shows the visualized data during early diastole. In contrast with Fig. 3a, the through-plane velocity was directed toward the ventricular apex, as indicated by the almost total preponderance of blue color. Because this occurred, during diastole, the mitral valve was open, which resulted in a continuous pathway between the ventricle and atrium. Therefore, no wall was drawn between these two chambers. Within the atrium, there also was an overall blue velocity directed from the atrium to the ventricle. The location of the mitral annulus, at which position the velocity is maximal, was hinted at by the very light blue or yellow portion of the raster images. Figure 3c shows the visualized data during early mitral valve closure. There still was flow from the atrium into the ventricle, as indicated by the light blue color at the location of the mitral valve. Within the ventricle, however, the flow no longer was apically orientated everywhere, because there are red, basally orientated velocity regions at the far side of the right three cut planes. These regions are located anterior to the anterior mitral leaflet in the LVOT region of the ventricle and indicate an intraventricular vortex. In the most apical slice, the flow still is apically orientated indicating that the vortex in the basal region of the heart did not extend to the apex. Figure 3d shows the visualized data at the end of diastole. The mitral valve closed, halting the flow of blood from the atrium to the ventricle. The through-plane velocity shows a bidirectionality with blue, apically orientated flow at the front of the images and red, basally orientated flow at the back. This indicates a vortex type flow, which, in contrast with the previous image, covers the entire ventricle. From the darkness of the colors, however, it also is evident that the velocities within this vortex were lower in this image than in the previous one.

As an alternative to the raster representation of the velocity, the cut plane function was used to visualize the velocity in vector form (Fig. 4). In Fig. 4, a cut plane was selected perpendicular to the four MR slices to visualize the ventricular inflow and outflow. The velocity vectors that are shown also have been interpolated, visualizing vectors between the MR slices. Figure 4a clearly shows the convergence of the flow toward the aorta at peak systole when the aortic valve on the right was open, and the mitral valve in the center was closed. Within the atrium, the flow of blood is in the opposite direction, toward the closed mitral valve, showing the S-wave of atrial inflow. As with the previous image, the mask data was used to show the outline of the ventricle and atrium. Notice, how-

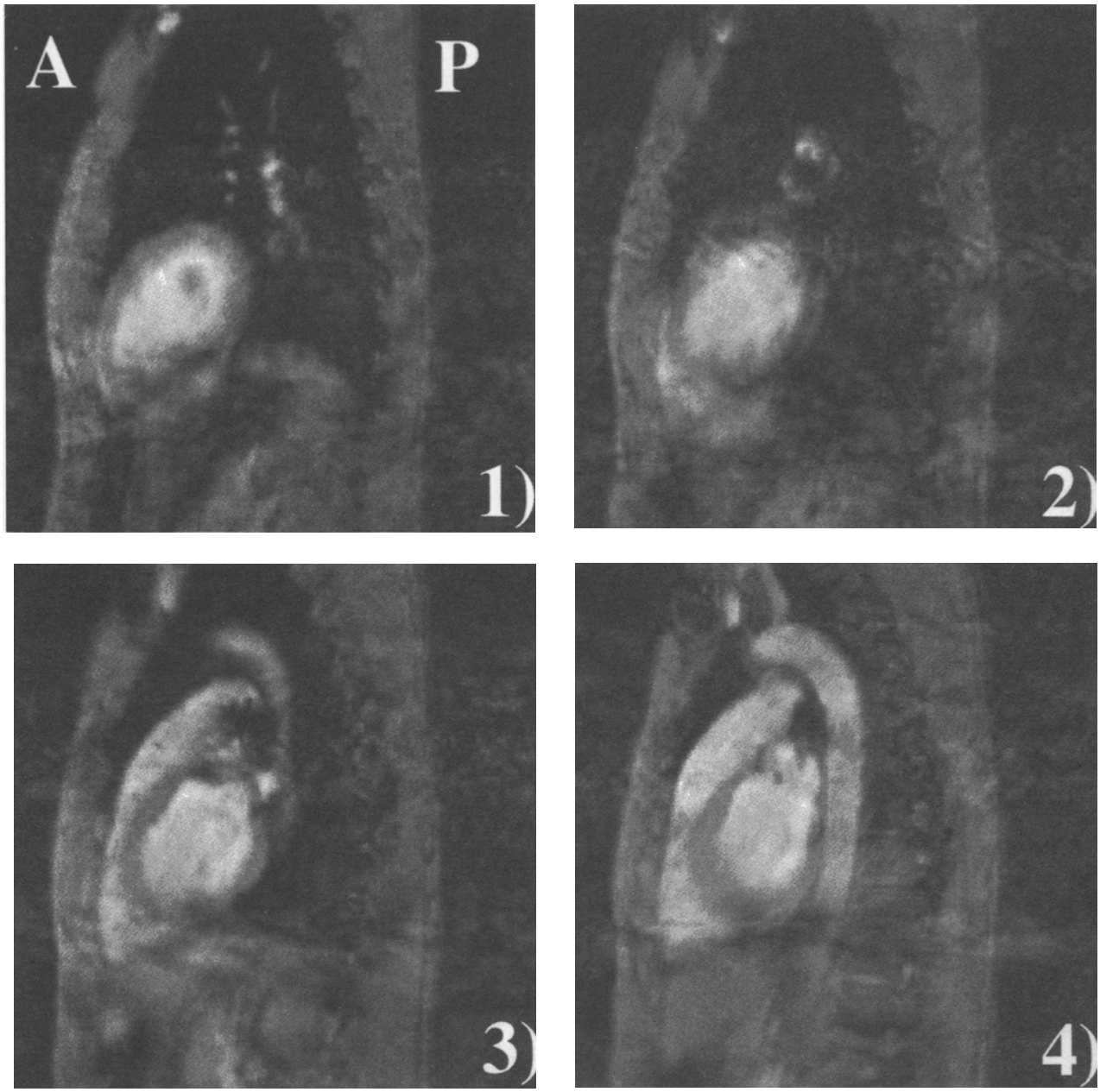

FIGURE 2. Magnitude images showing the anatomy in each of the four velocity slices 12 msec after the R-wave. LV, left ventricle; A, anterior; P, posterior. Images 1 to 4 progress from left to right of the subject.

ever, that the contour between the atrium and ventricle does not separate the two completely. Figure 4 (b and c) shows the vectors during early diastole and mitral valve closure. These figures show that the flow during early diastole was very strongly apically orientated throughout the ventricle and that this flow had a rounded profile. During mitral valve closure, the intraventricular vortex shown in Fig. 3 was seen, as was the mitral inflow. The vectors show that the velocity had increased and was now skewed toward the front of the images (posterior wall of the heart). The velocity vectors in Fig. 4, which represent all three components of velocity, show the general basal-apical motion of the blood during both systole and diastole. Relatively little motion of the blood was seen in the perpendicular direction.

In Fig. 5, the cut planes were used to show the velocity vectors in each of the MR planes for systole and diastole. From these images, the overall shape of the velocity profile can be gathered. For instance, the systolic image clearly shows the acceleration of the flow toward the aorta. Details or more subtle characteristics of the flow field, however, cannot easily be observed (Fig. 5), al-

though rotation of the images on the computer screen does give a better impression of the flow field than do these static photographs.

DISCUSSION

To a certain extent, the imaging portion of this project was simplified, because a multislice acquisition was made. In single slice imaging, the most difficult aspect often is locating a single plane that can describe enough of the flow field to be useful. This often takes time, especially when multiple angulations of the slice are needed. In contrast, when multislice images are acquired, it only is necessary to locate the slices so that they span the region of interest. The flow in particular planes can then be visualized by using the cut plane function after the data have been reconstructed on the computer. Therefore, multislice acquisitions are easier and quicker to set up than are single slice acquisitions. This is an important consideration because the acquisition time for a three-velocity component slice is approximately 20 mins. For these measurements, it was found that unangulated transverse and unangulated sagittal scans were suitable for the scout and velocity images, respectively.

The MRI parameters used for this study were chosen from past experience with imaging the human ventricle (25). The choices of slice thickness and field of view depend on the desired accuracy of the velocity measurement. Choosing a small slice thickness and small field of view yielded a smaller voxel size and therefore, a better spatial resolution within the ventricle. Unfortunately, the signal to noise ratio decreased as the voxel size decreased, resulting in a less accurate velocity measurement. A compromise must, therefore, be reached between accuracy of the velocity and spatial resolution. We found that a field of view of approximately 280 mm and slice thickness of between 6 and 10 mm gave good results (25). The spacing of the MR slices also is a parameter that can be varied to increase the spatial resolution of the data. In this experiment, the slices were 10 mm apart (center to center) resulting in a gap of 4 mm between slices. This spacing could have been decreased to obtain better spatial resolution, but so doing would have increased the examination time, because more slices would have been needed to cover the entire ventricle. We believed that this compromise was not worthwhile for the ventricular flow. In future studies, the time limitation may be removed because scanning methods currently are being developed to allow a single slice to be obtained in less than 1 min. However, the hardware and software used for this study were standard and can be used on any scanner.

The direct measurement of the velocity by MR and the acquisition of the MRI data by computer render the data analysis relatively straight forward. The only data manipulation necessary was the masking of the flow in the ventricle and the rearrangement of the data files into a format suitable for the visualization software. The masking of the flow in the ventricle was necessary because MR measures a velocity in every voxel, regardless of whether that velocity has any physical meaning. Such velocities tend to be irregular and, when represented in vector form, can confuse and obscure the correct velocity data. The masking of the image was performed by hand and, as a result, was relatively time consuming. Although there are methods to aid in the masking of the data, such as automated border detection algorithms, these methods are not of great use to these data because the contrast between the intraventricular blood pool and the myocardium may be small. This lack of contrast can occur for a number of reasons. First, the scanning method used may have been optimized for velocity acquisition and not for blood-myocardial contrast. Second, the signal magnitude of the blood may increase or decrease depending on a number of factors, such as motion, turbulence, and magnetic saturation, making it difficult to define a set threshold for the blood-myocardium interface. Finally, the slices may dissect the blood-myocardium interface at an oblique angle, thereby reducing the blood-myocardium contrast through the partial volume effect. However, masking by hand with use of the computer mouse can be accelerated when the mask from the previous cardiac phase is used for the current cardiac phase, because only the motion of the inner myocardial boundary must be taken into account. In addition, animation of the MR images can be used to aid in the masking, because motion can give an improved perception of the myocardial boundary.

After data analysis, the resultant masked data files were visualized with use of the commercial software package the Data Visualizer. One advantage of MR data is that they are rectangular in nature, and, therefore, only the pixel size and slice spacing are required to define the location of each voxel. This greatly simplified the file format and the visualization of the data. Within the Data Visualizer, the best tool for visualization was the cut plane function. This tool allowed the visualization of the data in one or more slices orientated through the three-dimensional data rectangle. Three methods were used with the cut plane function to visualize the data. The first was to create a contour of the mask data to show the edge of the ventricle and atrium. This was relatively straightforward because this edge is the only contour in the mask images. Initial attempts to visualize the anatomy of the heart used the MRI magnitude images and not the mask images. It was found, however, that these images, because of their poor contrast, location, and orientation, were too complex to provide a meaningful visualization of the heart structure. The second method used to visualize the data was a raster representation of the normal velocity.

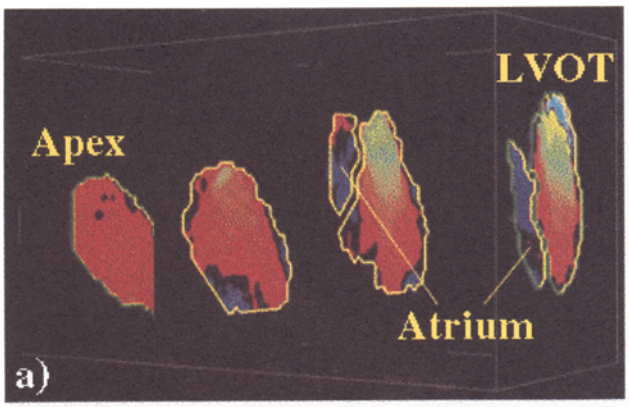

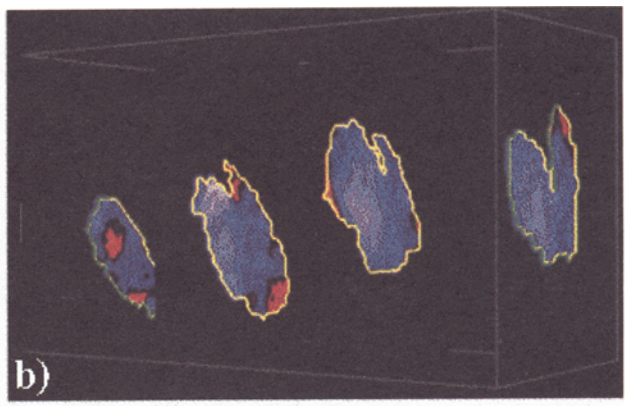

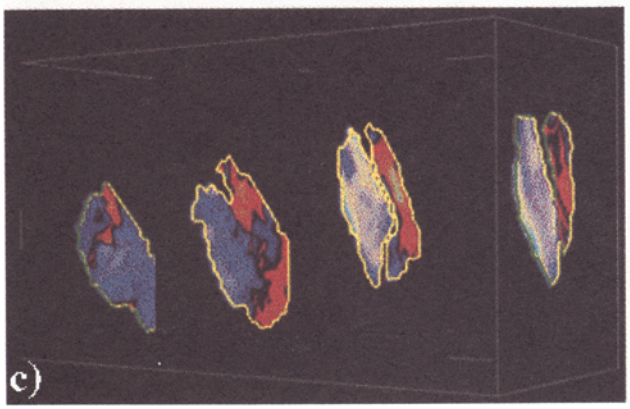

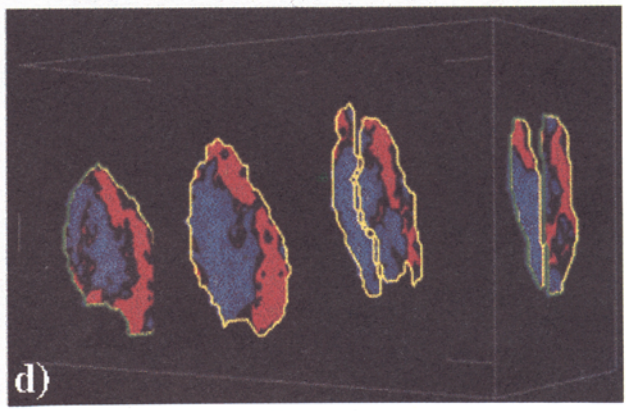

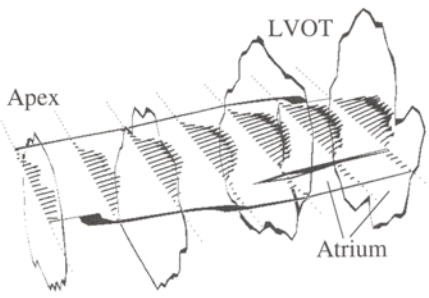

a)

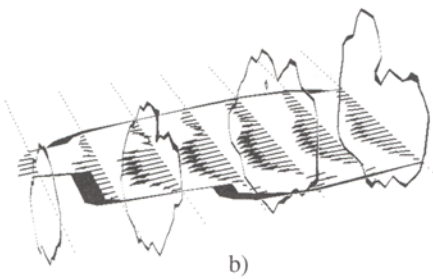

b)

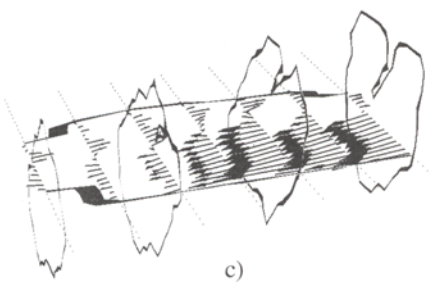

c)

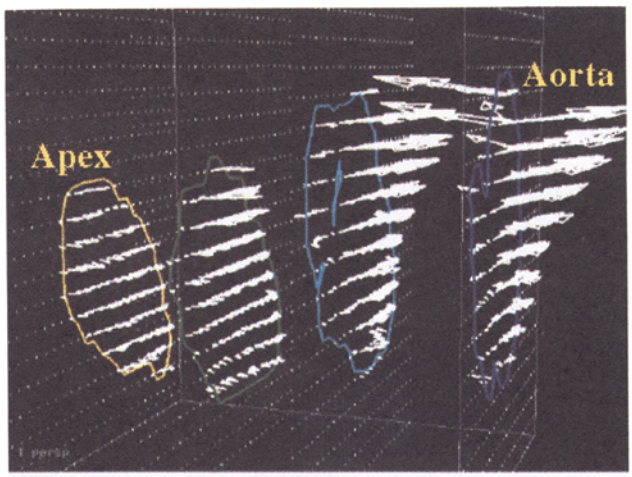

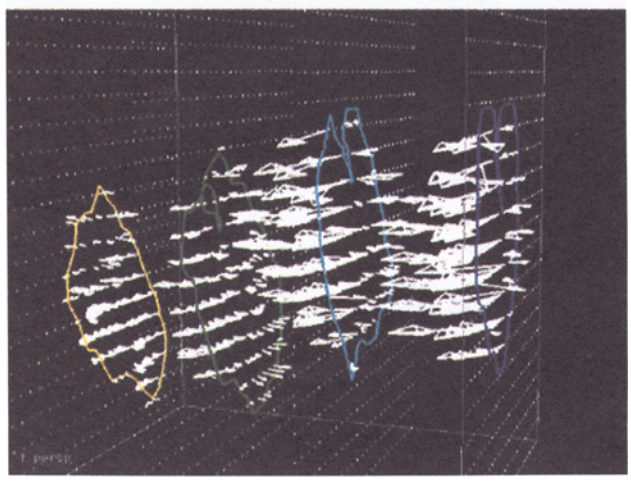

This type of visualization was useful because it simplified the data, allowing particular aspects of the flow to be seen. In this case, the normal velocity could be used to show the apical- to -basal motion of the blood in the ventricle. Because we found that this was the major direction of blood flow, this visualization gave a very good description of the flow, clearly showing the intraventricular vortex at the end of early mitral inflow. In cases, however, in which the flow is more complex, such a visualization may not yield a suitable flow description. The third type of visualization used was the vector plot of the velocity. Representing the velocity in vector form visualized both the velocity magnitude and direction and, therefore, was more descriptive of the flow. However, with this type, when there are many cut planes on display, the velocity vectors can tend to be confusing, especially when they overlap. For instance, in Fig. 5, the systolic flow is visualized well, giving a good impression of the convergence and acceleration of the flow toward the aortic valve. In contrast, however, the diastolic flow is not as well visualized, giving a poor impression of the intraventricular vortex shown on the raster images. By far, the best method to visualize the flow was to use a single cut plane containing velocity vectors and the mask contour. By using the mouse to move and rotate the cut plane around and through the three-dimensional data set, it was possible to investigate different aspects of the flow field. For instance, the examples shown in Fig. 4 clearly visualize the systolic outflow and diastolic vortex. In addition, by animating these images, the time-dependent motion of the blood through the atrium and ventricle can be seen clearly.

Previous single slice MRI and Doppler ultrasound imaging of the ventricular flow have shown that an intraventricular vortex is present during diastole (6,25). The three-dimensional reconstruction presented herein also was able to identify this vortex, but, in this case, the vortex could be visualized in three dimensions. This visualization revealed that the vortex, for this subject, was a vortex line rather than a vortex ring as has been suggested by others (3). The core of the vortex was aligned with the mitral valve leaflets so that flow was directed from the mitral valve along the posterior ventricular wall to the apex and from the apex along the intraventricular septum to the aortic valve. One possible explanation for the presence of a line vortex rather than a ring vortex is in the way in which the vortex was formed. The ring vortex hypothesis was derived from classical fluid mechanics, which showed that, when a bolus of fluid was impulsively injected into a stagnant chamber through a constrictive orifice, a ring vortex formed. In the case of early mitral inflow, however, it was suggested that these conditions did not exist. First, the fluid within the ventricle was not stagnant, but, in fact, was being driven apically by the relaxation of the ventricular walls and the opening motion of the mitral valve leaflets, Fig. 3b and 4b. Second, upon opening of the mitral valve, the leaflets, under normal function, extended very wide, even touching the intraventricular septum (25), to form a continuous chamber from the atrium to the ventricle. Figures 3b and 4b and Reference 25 show that, during this period of early filling, there was no, or at least very little, separation within the ventricle and, thus, no vortex was formed. These results show that the intraventricular vortex was created as the mitral valve leaflets began to close at, or just before, the peak in the mitral valve E-wave. The motion of both leaflets against the inflow generated vortices downstream (apical) of the leaflet tips. As time progressed, the vortex from the anterior leaflet dominated the one from the posterior leaflet and grew to fill the entire ventricle, producing a single intraventricular line vortex, Figs. 3d and 4c. This result suggests that the intraventricular flow depended on the mitral valve leaflets, and, therefore, simulations of ventricle flows should include realistic mitral valve geometries. During systole, the three-dimensional reconstruction of the flow showed that the blood accelerated toward the aorta from all regions of the ventricle. Such a flow is less complex than diastolic flow, because it has no recirculation regions, and is qualitatively similar to simulations of systolic ejection.

Compared with other methods for investigating intraventricular flow fields, three-dimensional MRI has the following advantages: it can directly measure the three-dimensional velocity vector; it is not hindered in the imaging by bone, etc., and, consequently, can obtain data in a slice orientated in any direction through the heart; it can simultaneously measure the anatomy; it can measure the temporal changes in these data; it obtains the data on actual hearts with no need for simplification; and it is non-invasive and safe. The disadvantages of MRI are the following: complex pressure fields are not obtained; it is difficult to image the mitral valve leaflets; the procedure triggers claustrophobia and is intimidating to some patients; and surgical wiring may hinder the imaging.

The effects of beat to beat variations on the measured

FIGURE 3. (Top 2 rows) Images of the normal velocity. Red, apical–basal velocity; blue, basal-apical velocity. a) Peak systole 73 msec after R-wave; b) Peak diastole, 397 msec after R-wave; c) mitral valve closure 467 msec after R-wave; d) end diastole 607 msec after R-wave. LVOT, left ventricular outflow tract.

FIGURE 4. (Bottom left) Velocity vectors in a cut plane perpendicular to the MR slices. a) Peak systole 73 msec after R-wave; b) start diastole 397 msec after R-wave; c) mitral valve closure 467 msec after R-wave. LVOT, left ventricular outflow tract.

FIGURE 5. (Bottom right) Velocity vectors in cut planes placed at the location of the MR slices. The top image is during systole, and the bottom image is during diastole.

velocity also must be considered. With the MRI phase velocity-encoding method, the data in an image were an average over a number of heartbeats. Beat to beat variations in the length of the cycle or the timing of the major heart events had the effect of smoothing out the velocities. When the imaging was triggered from the R-wave of the ECG, this smoothing was most noticeable at the end of the cycle, affecting the A-wave of mitral filling. In addition, when the heart rate was changing, the timing of the heart events could have varied between slices when multislice imaging is being used. These problems were reduced, however, when retrospective gating was applied. Retrospective gating works by averaging together data obtained at the same relative time in the heartbeat rather than data obtained at the same absolute time.

CONCLUSIONS

The measurement of the full time-dependent, three-dimensional flow in the left ventricle of a healthy human was performed and reconstructed on a computer. We found that the acquisition of the MRI data was relatively straightforward and required no special MRI pulse sequences or hardware. The data analysis also was relatively simple; it required only the masking of velocity to remove velocities from outside the heart and to provide an outline of the heart's anatomy. The resultant visualization was able to show the three-dimensional nature of the intraventricular flow field. The best visualization method was a cut plane in which the ventricular outline and the velocity vectors were displayed. This gave enough information to understand the flow, yet was not so complex as to clutter the image. The representation of a single velocity component in the raster form also was found to be useful. In more complex flows than those found herein, however, this method may be found lacking. Animation of the data was found to give an enhanced interpretation of the temporal nature of the data.

The intraventricular flow field was found to be simple during systole, with the blood accelerating toward the aorta from all regions of the ventricle. During early diastole, the flow also was relatively simple, with apically directed flow through the atrium and ventricle. However, during late diastole, reversed, basally directed flow was generated, which led to the formation of a large vortex in the ventricle. This vortex was a line vortex and not a ring vortex.

Finally, we have shown that MRI phase velocity measurements of the heart are possible and, therefore, are a potential new tool for investigating the full three-dimensional, time-dependent nature of ventricular hemodynamics.

REFERENCES

1. Back, L. H., D. G. Gordon, D. C. Ledbetter, R. H. Selzer, and D. W. Crawford. Dynamical relations for left ventricular ejection: Flow rate, momentum, force and impulse. *J. Biomech. Eng.* 106:54–61, 1984.
2. Beppu, S., S. Izumi, K. Miyatake, S. Nagata, Y.-D. Park, H. Sakakibara, and Y. Nimura. Abnormal blood pathways in left ventricular cavity in acute myocardial infarction. *Circulation* 78(1):157–165, 1987.
3. Bot, H., J. Verburg, B. J. Delemarre, and J. Strackee. Determinants of the occurrence of vortex rings in the left ventricle during diastole. *J Biomechanics* 23(6):607–615, 1990.
4. Delemarre, B. J., H. Bot, C. A. Visser, and A. J. Dunning. Pulsed Doppler echocardiographic description of a circular flow pattern in spontaneous left ventricular contrast. *J. Am. Soc. Echocardiogr.* 1(2):114–118, 1988.
5. Delemarre, B. J., C. A. Visser, H. Bot, and A. J. Dunning. Prediction of apical thrombus formation in acute myocardial infarction based on left ventricular spatial flow pattern. *J. Am. Coll. Cardiol.* 15(2):355–360, 1990.
6. Delemarre, B. J., C. A. Visser, H. Bot, H. J. D. Koning, and A. J. Dunning. Predictive value of pulsed Doppler echocardiography in acute myocardial infarction. *J. Am. Soc. Echocardiogr.* 2(2):102–109, 1989.
7. Firmin, D., G. L. Naylor, R. H. Klipstein, S. R. Underweed, R. S. O. Rees, and D. B. Longmore. *In-vivo* validation of MR velocity imaging. *J. Comp. Assist. Tomgr.* 11(5):751–756, 1987.
8. Garrahy, P. J., O. L. Kwan, D. C. Booth, and A. N. DeMaria. Assessment of abnormal systolic intraventricular flow patterns by Doppler imaging in patients with left ventricular dyssynergy. *Circulation* 82(1):95–104, 1990.
9. Georgiadis, J. G., M. Wang, and A. Pasipoularides. Computational fluid dynamics of left ventricular ejection. *Ann. Biomed. Eng.* 20:81–97, 1992.
10. Jacobs, L. E., M. N. Kotler, and W. R. Parry. Flow patterns in dilated cardiomyopathy: a pulsed-wave and color flow Doppler study. *J. Am. Soc. Echocardiogr.* 3(4):294–302, 1990.
11. Lanzer, P., W. McKibbin, D. Bohning, B. Thorn, G. Gross, G. Cranney, N. Nanda, and G. Pohost. Aortic iliac imaging by projection phase sensitive MR angiography: effects of triggering and timing of data acquisition on image quality. *Magn. Reson. Imaging* 8:107–116, 1990.
12. Matsuda, R., K. Shimizu, T. Sakurai, A. Fujita, H. Ohara, S. Okamure, S. Hashimoto, S. Tamaki, and C. Kawai. Measurement of aortic blood flow with MR imaging: comparative study with Doppler US *Radiology* 162:857–861, 1987.
13. McQueen, D. M., and C. S. Peskin. A three-dimensional computational method for blood flow in the heart. *J. Comput. Phys.* 81(2):372–395, 1989.
14. Meier, D., S. Maier, and P. Boesiger. Quantitative flow measurements on phantoms and on blood vessels with MR. *Magn. Reson. Med.* 8:25–34, 1988.
15. Mikell, F. L., R. W. Asinger, K. J. Elsperger, W. R. Anderson, and M. Hodges. Regional stasis of blood in the dysfunctional left ventricle: echocardiographic detection and differentiation from early thrombosis. *Circulation* 66(4): 755–763, 1982.
16. Morvan, D., F. Cassot, and R. Pelissier. Simulation numerique do l'ecoulement intraventriculaire par une methode

particulaire J. Mecanique Theorique Appliquee 6(4):489–509, 1987.
17. Pelle, G., J. Ohayon, and C. Oddou. Trends in cardiac dynamics: towards coupled models of intracavity fluid dynamics and deformable wall mechanics. *J. Physics* III 4: 1121–1127, 1994.
18. Peskin, C. S., and D. M. McQueen. Modeling prosthetic heart valves for numerical analysis of blood flow in the heart. *J. Comput. Phys.* 37(1):113–132, 1980.
19. Ridgeway, J. P., and M. A. Smith. A technique for velocity imaging using magnetic resonance imaging. *Br. J. Radiol.* 59:603–607, 1986.
20. Schoephoerster, R. T., C. L. Silva, and G. Ray. Finite analytic model for left ventricular systolic flow dynamics. *J. Eng. Mech.* 119(4):733–747, 1993.
21. Schoephoerster, R. T., C. L. Silva, and G. Ray. Evaluation of left ventricular function based on simulated systolic flow dynamics computed from regional wall motion. *J. Biomech.* 27(2):125–136, 1994.
22. Stugaard, M., O. A. Smiseth, C. Risoe, and H. Ihlen. Intraventricular early diastolic filling during acute myocardial ischemia: assessment by multigated color M-mode Doppler echocardiography. *Circulation* 88(6):2705–2713, 1993.
23. Sun, Y., D. O. Hearshen, G. W. Rankin, and A. M. Haggar. Comparison of velocity-encoded MR imaging and fluid dynamic modeling of staedy and disturbed flow. *J. Magn. Reson. Imaging* 2:443–452, 1992.
24. Taylor, T. W., H. Okino, and T. Yamaguchi. Three-dimensional analysis of left ventricular ejection using computational fluid dynamics. *J. Biomech. Eng.* 116:127–130, 1994.
25. Walker, P. G., G. B. Cranney, M. B. Scheidegger, G. Waseleski, G. M. Pohost, and A. P. Yoganathan. A semiautomated method for noise reduction and background phase error correction in NMR phase velocity data. *J. Magn. Reson. Imaging* 3:521–530, 1993.
26. Walker, P. G., S. Oyre, E. M. Pedersen, A. P. Yoganathan. The accuracy of MR phase encoding measurements downstream of a mechanical heart valve: a comparison with LDA (Abstract). 12th Annual Meeting, Society of Magnetic Resonance Imaging, New York, 1993.
27. Walker, P. G., E. M. Pedersen, S. Oyre, L. Flepp, S. Ringgaard, R. S. Heinrich, S. P. Walton, J. M. Hasenkam, H. S. Jorgensen, and A. P. Yoganathan. Magnetic resonance velocity imaging: a new method for prosthetic heart valve study. *J. Heart Valve Dis.* 4:296–307, 1995.
28. Yoganathan, A. P., J. D. Lemmon, Y. H. Kim, P. G. Walker, R. A. Levine, and C. C. Vesier. A computational study of a thin-walled 3D left ventricle during early systole. *J Biomech. Eng.* 116:307–314, 1994.